CrossMark

ORIGINAL ARTICLE

Segmentation of weather radar image based on hazard severity using RDE: reconstructed mutation strategy for differential evolution algorithm

Meera Ramadas[1] · **Millie Pant**[2] · **Ajith Abraham**[3] · **Sushil Kumar**[1]

Abstract Weather describes the condition of our atmosphere during a specific period of time, and climate represents a composite of day to day weather over longer period of time. Climatology attempts to analyze and explain the impact of climate so that the society can plan accordingly. Climatology analysis is often done on radar images representing various climatic conditions. These images contain varying scale of severity for any specific climatic parameter of study. The climatologists often find it convenient to analyze climatic conditions if tools are available to segment the weather images based on the severity scale which is represented by different colors. Segmentation of the weather radar image is also used for automated analysis of weather conditions. Differential evolution (DE) approach instead is used for fast selection of optimal threshold. In present paper, we have applied DE with multilevel thresholding for weather image segmentation which results in minimum computational time and excellent image quality. A new mutation strategy for DE named reconstructed differential evolution (RDE) strategy is suggested for better performance over image segmentation. Using fuzzy entropy and RDE for multilevel thresholding provides better results in comparison with last suggested methods.

✉ Meera Ramadas
meera_mgr@rediffmail.com

1 Amity University Uttar Pradesh, Noida, India

2 Department of Applied Science and Engineering, Indian Institute of Technology Roorkee, Roorkee, India

3 MIR Labs, Auburn, WA, USA

1 Introduction

Weather surveillance radar is used to locate the motion, movement and type of precipitation. The weather radar images provide a map view of reflected particles for specific area around the radar. With the varying intensity of precipitation, different color codes are used for its representation. With the help of these radar images, we can predict the climatic conditions. High-resolution satellite images have become a good source of information for weather forecasting. Efficient extraction and processing of useful data can improve the weather forecasting. By splitting the images according to color code, the specific hazard type can be viewed and depending on the intensity, the corresponding alerts can be given to public for their safety.

Thresholding is a basic technique of image segmentation which converts the image into foreground and background images. Thresholding on colored images is done by manipulating the color components based on color spaces. Image thresholding is classified as unsupervised learning and such issues can be solved using evolutionary algorithms. The most robust evolutionary algorithm DE was introduced by Storn and Price [1] algorithm that follows the concepts of evolutionary algorithms like mutation, selection and reproduction. DE remains straightforward, stochastic, population-based algorithm that helps solving optimization problem. The efficiency and performance of DE are determined based on the control parameters and the trial vectors generation strategy being used. Numerous variants of DE are designed by changing these trial vector strategy and control parameters. In DE algorithm, population size, crossover constant and the mutation scale factor F are the three control parameters being used.

Reconstructed differential evolution strategy (RDE) uses three different mutation scale factors to help image

🙾 Springer

segmentation efficiency. Suggested RDE strategy is compared with the other classical variants to confirm better efficiency. To verify the efficiency of RDE for image thresholding, we have applied it on segmenting the weather images based on specific climatic condition. Based on fuzzy entropy, multilevel image thresholding is then used along with the differential evolution approach to perform the image segmentation. The first section of the paper explains the concept of thresholding and entropy-based thresholding. The second section details the differential evolution approach and the proposed mutation strategy. The rest explain the implementation of RDE in multilevel thresholding and results.

2 Related literature study of thresholding using evolutionary algorithms

Roula et al. [2] stated the problems of automatic segmentation of nuclei in histopathological images and for solving global optimization problem, an active contour-based evolutionary approach was proposed. Results show the efficiency of the method. Omran et al. [3] developed a clustering method based on DE which applied to unsupervised classification and segmentation of images. Rahnamayan et al. [4] introduced a new optimization-based thresholding approach using differential evolution. This method performs better than the Kittler algorithm of thresholding. Aslantas et al. [5] explained the usage of different DE algorithms aimed at segmenting the wounds on skin. Developed technique removes the disadvantages of k-means clustering. Rahnamayan et al. [6] introduced micro-opposition-based DE (micro-DE) which performs better than Kittler algorithm in sixteen test images. Hasan et al. [7] aimed on pulling out chain codes of thinned binary image using DE and PSO. Milad et al. [8] introduced a blend of hierarchical evolutionary algorithm (HEA) and multilevel thresholding algorithm for segmenting magnetic resonance images. On the basis of an automatic multilevel thresholding approach, HEA uses an unsupervised clustering technique. The results were evaluated, and performance was validated.

Kumar et al. [9] combined the Otsu method with differential evolution technique to select the optimum threshold value. The results were verified by testing the method on four different images. Li et al. [10] on the basis genetic algorithm for water area extraction during flood events and two-dimensional entropy introduced a type of image processing. In the areas of water monitoring, this technique was found to be quite efficient and reliable. Sarkar and Das [11] for improving separation between objects presented a 2D histogram-based multilevel thresholding approach. The results were found to be superior to the results achieved from 1D histogram-based technique for bilevel thresholding.

Paul et al. [12] provided image compression technique built on histogram for multilevel thresholding. Various image quality techniques were used for image comparison. Specific application of the method was also proposed. Ochoa-Montiel [13] gave the thresholding of biological images using multiobjective optimization technique. In the paper, a combination of Shannon technique with Otsu thresholding has been used for inter- and intra-class. Results show less computational efforts for this technique. Allaoui et al. [14] proposed a technique to solve thresholding problem, initialization and sensitivity to noise. The suggested method is on region growing and evolutionary approach. The literature review provides works based on evolutionary algorithm used on images are discussed. Research is still going on to develop more robust and efficient techniques based on evolutionary approaches to solve optimization problems like image segmentation.

3 Multilevel image thresholding

Thresholding is the simplest technique of image segmentation for gray scale image to create binary images. Designating separate RGB components of the image use for color image thresholding. The various techniques used for thresholding are: histogram shape, entropy, clustering- and attribute-based method, local method and spatial method.

Depending on number of image segments, thresholding is of two types called bilevel and the multilevel. In the case of bilevel thresholding, the image segmentation is done in two different regions. Threshold level is defined by the term 'T.' One region holds the pixel having gray value larger than 'T,' and the other region holds gray values lesser than 'T.' The first region is known as object pixels, and the other is known as background pixels. In multilevel thresholding, the foreground and background objects are segregated into non-overlapping sets which aids in segmenting the gray scale image into different sections. It is a type of clustering technique in which the gray level samples are grouped into two sections as background and foreground. In this method, different values are assigned between different ranges of threshold levels. The number of thresholds is stated in advance.

Texture of the input image can be characterized by using a statistical measure of randomness called entropy. Entropy of an image can be expressed as:

$$\text{Entropy} = -\sum_{j}^{m} p_j * \log_2(p_j). \tag{1}$$

Here, p_j is the probability of j and m in gray scale level becoming equal to the difference in-between two neighboring pixels. Entropy of an image provides the level of

information for the study of image. Low entropy has little contrast between pixels and large run of pixels. Run is the sequence of pixels of same color. So, in low entropy, the sequence of pixels with same color will be more. Images with low entropy have lesser information and can be easily compressed. A flat image has zero entropy. High entropy has very high contrast between pixels and cannot be compressed as low entropy images.

The measure of uncertainty and entropy over a fuzzy set of an image is referred as fuzzy entropy. Consider an image Y of size $I \times J$. Fuzzy entropy of an image is denoted as:

$$\text{Fuzzy entropy} = \frac{1}{IJ \ln 2} \sum_{i=1}^{I} \sum_{j=1}^{J} S_n(\mu_Y(y_{ij})), \tag{2}$$

where $\mu_Y(y_{ij})$ represents the measure of a property of image like pixel brightness and S_n denote the Shannon's function denoted as:

$$S_n(\mu_Y(y_{ij})) = -\mu_Y(y_{ij}) \ln \mu_Y(y_{ij}) - (1 - \mu_Y(y_{ij})) \ln(1 - \mu_Y(y_{ij})). \tag{3}$$

If the fuzzy entropy is larger, greater will be the information within that fuzzy set. Y is then segmented into background and object pixels using the fuzzy threshold b:

$$y_{ij} = \begin{cases} 0 & y_{ij} < b \\ 255 & y_{ij} \geq b \end{cases}, \tag{4}$$

where $i = 1, 2, 3, \ldots I$ and $j = 1, 2, 3, \ldots j$ In this paper, we have used fuzzy entropy-based technique to perform the thresholding of the color image.

4 Classical DE algorithm

A defined number of vectors are evolved over time from a search space of n-dimensions of likely solutions to derive local minima of the objective function. A specified number of vectors being obtained over time within the search space are arbitrarily recognized. DE use population of NP candidate's solution designated as $X_{i,j}$ where $i = 1, 2, \ldots NP$ where index i signify population and G symbolizes generation of population. Differential evolution algorithm depends on the three operations: mutation, selection and reproduction.

Mutation It determines the weighted difference among the vectors in population. For any specified parameter $X_{i,G}$, we are arbitrarily choosing three vectors $X_{r1,G}$, $X_{r2,G}$ and $X_{r3,G}$ such that r_1, r_2, r_3 are dissimilar. Then, the donor vector $V_{i,G}$ is computed as:

$$V_{i,G} = X_{r1,G} + F \times (X_{r2,G} - X_{r3,G}). \tag{5}$$

Here, the mutation factor F is a constant within [0,1].

Crossover This process also termed as recombination comprises of effective solutions into the population. Trial vector $U_{i,G}$ is aimed at target vector $X_{i,G}$ with binomial crossover. Within a probability $C_r \in [0, 1]$, the component of donor vector moves into trial vector. Crossover probability C_r is selected along with population size $NP \geq 4$.

$$U_{j,i,G+1} = \begin{cases} V_{j,i,G+1} & if\ rand_{i,j}[0,1] \leq\ or\ if\ j = I_{rand.} \\ X_{j,i,G+1} & if\ rand_{i,j}[0,1] \leq\ or\ if\ j \neq I_{rand.} \end{cases} \tag{6}$$

Here, $rand_{i,j} \approx \cup[0,1]$ and I_{rand} being the random integer within $1, 2, \ldots N$.

Selection Population proposed for succeeding generation is selected from vectors within the current population and the successive trial vectors. Target vector $X_{i,G}$ is harmonized with trial vector $V_{i,G}$ with the smallest value of function and is incorporated in resulting generation.

$$X_{i,G+1} = \begin{cases} U_{i,G+1} & if\ f(U_{i,G+1}) \leq f(X_{i,G}) \quad where\ i = 1, 2, \ldots N \\ X_{i,G} & otherwise. \end{cases} \tag{7}$$

Mutation, crossover and selection operations will continue till some ending criteria stands attained.

5 RDE mutation strategy

In RDE, the mutation strategy has three control parameters: a constant parameter F, a variable $N1$ and $N2$, where $N2$ is a complement value of $N1$. Both variables $N1$ and $N2$ have the value (0, 1), one will be generated randomly and second will take a complement value of the first variable. By involving the best solution vector, proposed strategy coincides faster as compared to the traditional strategies which have only random vectors. This strategy also uses variables X_{r1}^G, X_{r2}^G, X_{r3}^G which are chosen at random. The parameter F known as mutation factor takes a constant value between (0, 1). The usage of mutation factor F has been used in traditional strategies also. As we are taking three different control parameters, the value of donor vector is improved greatly. In this strategy, the weighted difference of solution vectors is found using $N1$ and $N2$. The difference of these values is obtained, and the weighted difference of this value is added to the solution vector. As the mutation strategy of DE is changed by using three control parameters, RDE is a hybrid of classical DE algorithm. By changing the mutation strategy of the traditional DE algorithm with RDE, the efficiency of the classical DE algorithm is improved. The proposed strategy is given as:

$$V_{i,G} = X_{r1}^G + F \times (N1 \times (X_{best}^G - X_{r2}^G) - N2 \times (X_{best}^G - X_{r3}^G)). \tag{8}$$

By increasing the number of control parameters to three, the convergence speed is increased profoundly and avoids premature convergence. Also, these control parameters prevent the RDE algorithm from collecting the neighborhood of global best individuals. As there are three different control parameters, the value of donor vector is improved greatly and hence the efficiency of RDE algorithm is enhanced profoundly in comparison with classical DE algorithm.

6 Experimental results

RDE was executed on i7 core processor, 64-bit operating system via MATLABr2008b to perform a relative analysis to original DE algorithm. Five different traditional mutation strategies of DE algorithm are considered for comparing the results and for showing the exact information. Fifteen standard functions are considered, and the results from various mutation strategies are obtained by fitting the value-to-reach and number of iterations. Value-to-reach (VTR) is referred to as global minimum or maximum for a function to stop the optimization if it is reached. The results are tabularized for evaluation with the prevailing algorithms.

On the basis of the best value subsequent to 50 runs (vtr = 1.e−015):

A relative investigation was executed, and in-depth study was performed on individual method. By assigning the size and value-to-reach (VTR), the best value, number of function evaluation (NFE) and the CPU time of diverse function approaches were recorded. RDE gave best value for greatest number of standard functions. The best results obtained for each benchmark functions are indicated in bold format. To perform the statistical analysis on the results from Table 1, Friedman's test was implemented and the values obtained were formulated. Table 2 denotes the results attained from the test, and Table 3 depicts the rank of the various mutation strategies used based on best value obtained.

Tables 2 and 3 show that RDE has significant performance in comparison with the existing mutation strategies. The rank obtained based on best value is comparatively better for RDE. These rankings obtained based on Freidman's test justify the efficiency of RDE strategy.

7 Multilevel thresholding with RDE strategy

In the paper, we have introduced the DE approach to fuzzy entropy-based thresholding. In this approach, we have used the RDE mutation strategy for DE as given in Eq. 8. Using Eq. 2, the fuzzy entropy provides the fitness function meant for the DE algorithm. The flowchart for the proposed work is given in Fig. 1.

8 Test results on image thresholding

The proposed RDE strategy was combined with the fuzzy entropy approach to perform multilevel image thresholding. This method was applied on two sets of weather radar images. The results obtained were compared with the results obtained from multilevel thresholding using classical DE approach. Higher the entropy, better the information captured in the image. The entropy value obtained for RDE is better than the value obtained using classical DE. Optimal threshold value and CPU time taken for segmentation of image 1 and 2 are better for RDE. Hence, the quality of segmented image is better for RDE than the classical DE. The improvement in quality of image is due to the inclusion of new control parameters in DE algorithm which resulted in creation of the new hybrid RDE. The values for threshold, entropy and CPU time are computed and tabulated in Table 4. The original image and the images after thresholding using DE and RDE technique are shown in Figs. 2 and 3. The overall results obtained demonstrate the proposed RDE strategy gives improved results for multilevel thresholding in comparison with classical DE approach.

The above results clearly indicate that the values obtained for RDE strategy-based thresholding is much better compared to the results obtained using DE strategy. Two sample weather radar images were taken from www. wunderground.com, and the multilevel thresholding was performed on these images. The image after thresholding was segmented based on the specific hazard severity. Samples of rainfall image and snowfall results obtained are given in Figs. 2 and 3.

Color enhancements are seen in a radar image to help in interpretation. The specific colors are compared with the standard color bar to identify the hazard severity. Different colors on the image depict different intensities of the weather condition. The violet/pink color bar shows the extreme weather condition of snow, rain or hail in an area. The red color bar shows an intense weather condition. The yellow color bar shows a very heavy precipitation level, and the green color bar shows heavy condition. Light blue color bar shows moderate climatic conditions. By clustering the images separately according to the specific hazard severity, it is easy to identify and predict the specific weather condition across the plains.

Table 1 Comparative analysis for best value obtained for diverse functions

Function	D	VTR	DE					RDE	Significance
			DE/best/1	DE/rand/1	DE/best-to-rand/1	DE/best/2	DE/rand/2		
Sphere	50	1.e−015	9.714e−016	6.891e−016	7.454e−016	9.766e−016	7.127e + 0	**6.62e−016**	+
	25	1.e−015	9.324e−015	9.335e−015	9.59e−015	9.442e−015	6.912e + 000	**8.46e−014**	+
	25	1.e−014	8.45e−016	9.899e−016	6.23e−016	9.7e−016	**2.517e−001**	8.26e−015	−
Beale	50	1.e−015	3.126e−016	**2.312e−016**	3.718e−016	7.56e−016	7.723e−016	7.67e−016	−
	25	1.e−015	4.226e−015	7.712e−015	**1.12e−015**	1.316e−017	7.25e−015	4.4e−015	−
	25	1.e−014	5.89e−016	2.456e−016	3.78e−016	9.673e−016	3.89e−016	**6.7e−015**	+
Booth	50	1.e−015	3.45e−016	2.045e−016	6.067e−016	7.057e−016	8.23e−016	**9.21e−015**	+
	25	1.e−015	1.80e−015	7.45e−016	**1.92e−015**	2.745e−015	6.447e−015	2.6e−015	−
	25	1.e−014	3.27e−016	5.887e−016	1.746e−016	5.89e−016	3.47e−016	**5.5e−015**	+
Schwefel	50	1.e−015	**−1.812e + 003**	−2.245e + 003	**−7.834e + 001**	−1.281e +003	**−1.667e +003**	**−3.32e + 002**	NA
	25	1.e−015	−4.322 + 002	−4.78e + 002	−1.667e + 003	−4.467e + 003	−1.45e + 003	−1.42e + 003	NA
	25	1.e−014	−5.61e + 002	−2.4e + 003	−6.34e + 002	−4.83e + 003	−2.44e + 003	−1.7e + 003	NA
Michlewicz	50	1.e−015	**−7.654e +00**	**−7.231e + 00**	**−7.42e + 00**	**−6.956 e + 00**	**−6.885 e + 00**	**−1.13e + 001**	NA
	25	1.e−015	−7.689e +00	−7.664e + 00	−6.787e + 00	−7.235e + 00	−6.898 e + 00	−6.6e + 00	NA
	25	1.e−014	−1.123e + 001	−1.22e + 001	−1.231e + 001	−1.214e + 001	−1.122e + 001	−1.1e + 001	NA
Schaffer N.2	50	1.e−015	6.56e−016	8.788e−016	4.343e−016	6.455e−016	8.787e−016	**6.66e−015**	+
	25	1.e−015	1.323e−015	1.433e−015	6.566e−016	5.43e−015	**1.233e−015**	0	−
	25	1.e−014	6.656e−016	8.878e−016	0	8.858e−016	6.626e−016	1.55e−015	+
Schaffer N.4	50	1.e−015	3.045e−015	2.89e−001	2.912−001	2.923e−001	2.879e−001	**2.85e−001**	+
	25	1.e−015	2.92e−001	2.92e−001	2.92e−001	2.923e−001	2.879e−001	2.92e−001	NA
	25	1.e−014	2.92e−001	2.92e−001	2.92e−001	2.92e−001	2.92e−001	2.92e−001	NA
HimmelBlau	50	1.e−015	1.56e−016	8.045e−016	3.783e−016	9.132e−016	**1.456e−016**	4.38e−016	−
	25	1.e−015	4.873e−015	4.432e−015	**1.9102e−015**	3.945e−015	5.114e−015	3.2e−016	−
	25	1.e−014	**6.39e−016**	7.28e−017	5.75e−017	7.07e−016	7.77e−016	9.6e−016	−
Bird	50	1.e−015	**−1.025e + 002**	**−1.057e + 002**	**−1.045e + 002**	**−1.055e + 002**	**−1.023e + 002**	**−1.04e + 002**	NA
	25	1.e−015	−9.313e + 001	−1.034e + 002	−1.056e + 002	−1.024e + 002	−1.034e + 002	−1.03e + 002	NA
	25	1.e−014	−1.029e + 002	−1.056e + 002	−1.047e + 002	−1.035e + 002	−1.018e + 002	−1.06e + 002	NA
Extended Cube	50	1.e−015	3.21e−015	4.88e−006	6.21e−008	1.83e−005	2.58e + 00	**2.04e−006**	+
	25	1.e−015	5.501e−008	5.112e−005	7.110e−008	**1.63e−005**	2.82e + 009	2.156e−006	−
	25	1.e−014	1.46e−007	2.84e−010	1.26e−007	9.34e−011	2.61e−014	**1.65e−006**	+
Ackeley	50	1.e−015	7.16e−015	**6.36e−012**	7.89e−015	3.53e−013	3.05e + 00	4.4e−015	−
	25	1.e−015	7.89e−015	5.01e−015	7.89e−015	3.49e−015	3.113e + 00	**4.4e−014**	+
	25	1.e−014	7.79e−015	6.23e−013	7.89e−015	9.22e−014	**7.09e−014**	7.9e−015	−

Table 1 continued

Function	D	VTR	DE						RDE	Significance
			DE/best/1	DE/rand/1	DE/best-to-rand/1	DE/best/2	DE/rand/2			
Gold	50	1.e−015	3.00e+00	3.00e+00	3.00e+00	3.00e+00	3.00e+00		3.0e+00	NA
	25	1.e−015	3.00e+00	3.00e+00	3.00e+00	3.00e+00	3.00e+00		3.0e+00	NA
	25	1.e−014	3.00e+00	3.00e+00	3.00e+00	3.00e+00	3.00e+00		3.0e+00	NA
Griewank	50	1.e−015	9.89e−016	9.79e−016	**1.56e−013**	6.46e−013	1.04e+00		9.79e−016	−
	25	1.e−015	**1.467e−002**	9.114e−015	7.788e−015	5.17e−009	1.16e+00		6.6e−016	−
	25	1.e−014	**1.13e−002**	8.78e−016	7.55e−016	8.781e−016	6.67e−011		9.65e−015	−
Rastrigin	50	1.e−015	1.69e+001	1.123e+002	7.37e+001	1.18e+002	1.42e+002		8.04e+001	NA
	25	1.e−015	3.631e+001	1.081e+002	8.27e+001	1.627e+002	1.634e+002		6.61e+001	NA
	25	1.e−014	6.18e+001	9.82e+001	6.47e+001	1.037e+002	1.19e+001		7.17e+001	NA
Rosenbrock	50	1.e−015	9.56e−016	**1.04e−008**	7.78e−016	3.89e−009	1.067e+005		7.48e−016	−
	25	1.e−015	3.78e+00	1.303e−008	6.89e−015	**1.46e−011**	7.25e+004		8.52e−016	−
	25	1.e−014	9.45e−016	**2.13e−012**	3.59e+00	7.45e+005	3.41e+008		9.7e−014	−

Table 2 Statistical analysis using Friedman's test of RDE

N	50
Chi-sq	23.47
Df	5
Asymptotic significance	0.0003

Table 3 Ranks of the different strategies with RDE

Strategies	Mean rank on best value
DE/best/1	2.8
DE/rand/1	3.1
DE/best-to-rand/1	2.71
DE/best/2	4.13
DE/rand/2	5.1
RDE	2.83

Read the image

↓

Initialize the number of thresholds required

↓

Compute the histogram value of the image and fitness function using fuzzy entropy

↓

Apply RDE approach with fuzzy entropy

↓

Calculate the threshold value and apply it on image
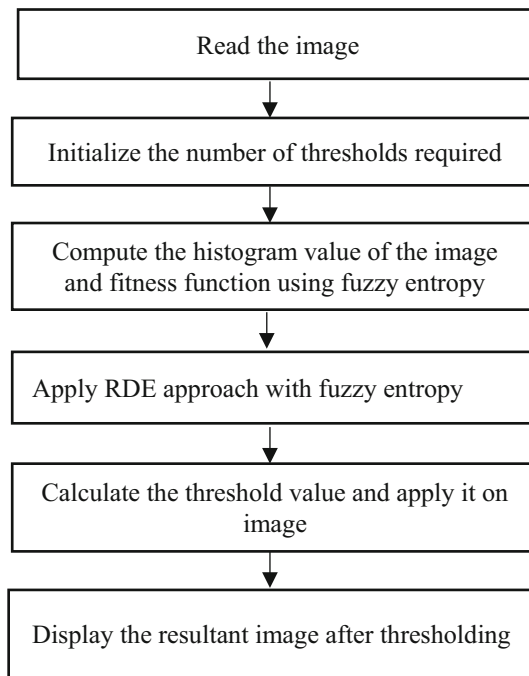
↓

Display the resultant image after thresholding

Fig. 1 Flow chart for multilevel thresholding using RDE

From the above resultant images, it is easy to identify the regions of extreme and intense weather conditions. In the original image, it is not very easy to see at a glance if a case of extreme condition is occurring on any specific land area. After separating the images based on color bar, the area for extreme and intense conditions is identified easily. In Fig. 4, for example, the image for extreme condition shows only pink on the corresponding effected area,

Table 4 Values obtained from images after thresholding

Image	Methods used	Entropy value	Threshold value	CPU time
Image 1	DE-based thresholding	0.98	0.38	12.43
	RDE-based thresholding	0.99	0.42	11.7
Image 2	DE-based thresholding	0.803	0.48	17.02
	RDE-based thresholding	0.818	0.49	14.3
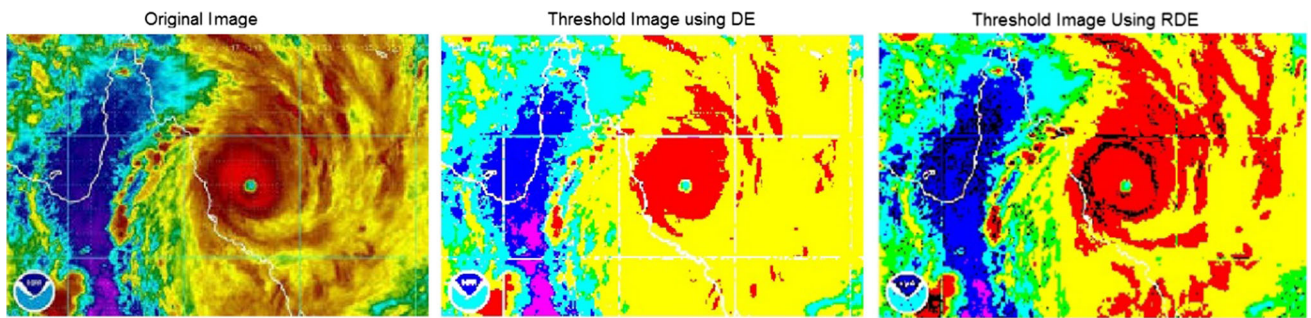
Fig. 2 Original and threshold image of sample image 1
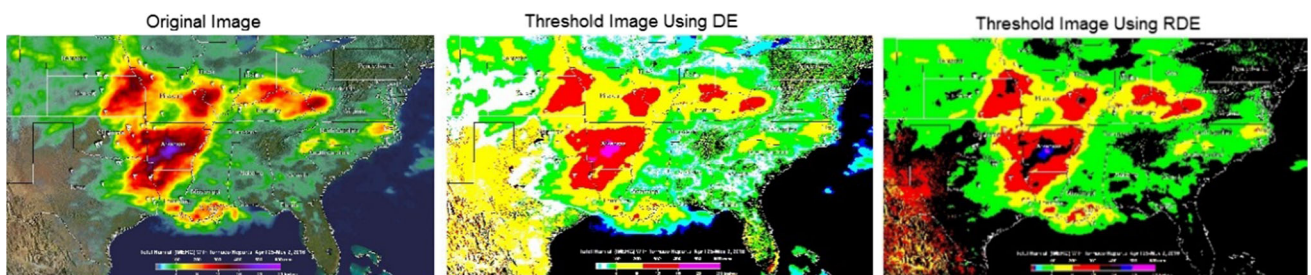
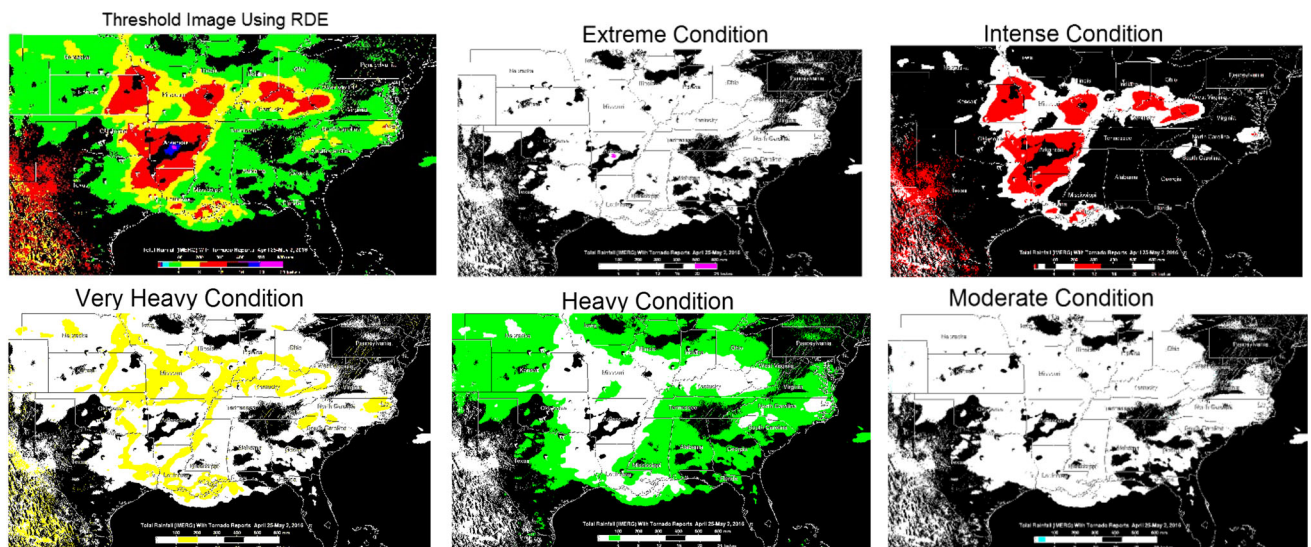**Fig. 3** Original and threshold image of sample image 2

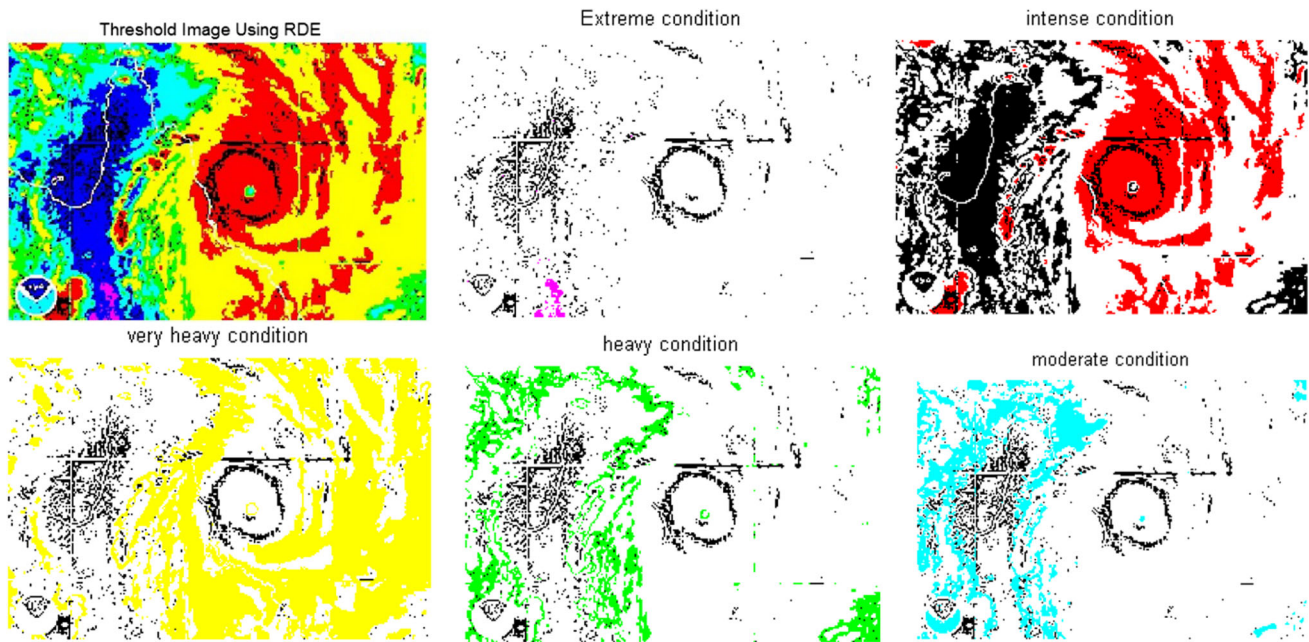**Fig. 4** Sample image 2 segmented based on hazard severity

Fig. 5 Sample image 1 segmented based on hazard severity

whereas for moderate condition the image easily depicts that no region on the map is having that specific climatic condition (Fig. 5).

9 Conclusion

Herein the proposed work, reconstructed mutation strategy was implemented in DE algorithm and results being compared to prevailing mutation strategies. The comparative study shows better results for RDE. RDE applied to multilevel thresholding based on fuzzy entropy. The thresholding results were found to be better for RDE strategy in comparison with classical DE approach. The threshold image was further segregated based on the specific hazard level. From our study, it is seen that RDE strategy performs much better in comparison with other strategies. Currently, the strategy has been applied for weather forecasting. An extension of the work can be done to apply this technique for medical image processing, land topology, image enhancement and other image processing areas.

Compliance with ethical standards

Conflict of interest The authors declare that there is no conflict of interest.

References

1. Storn R, Price K (1997) Differential evolution–a simple and efficient heuristic for global optimization over continuous spaces. J Global Optim 11(4):341–359

2. Roula MA, Bouridane A, Kurugollu F (2004) An evolutionary snake algorithm for the segmentation of nuclei in histopathological images. In: 2004 International Conference on Image Processing, 2004. ICIP'04. vol. 1, IEEE, pp. 127–130

3. Omran MGH, Engelbrecht AP, Salman A (2005) Differential evolution methods for unsupervised image classification. In: 2005 IEEE Congress on Evolutionary Computation, vol. 2, IEEE, pp. 966–973

4. Rahnamayan S, Tizhoosh HR, Salama MMA (2006) Image thresholding using differential evolution. In: International conference of image processing, computer vision and pattern recognition, pp. 244–249

5. Aslantas V, Tunckanat M (2007) Differential evolution algorithm for segmentation of wound images. In: IEEE International Symposium on Intelligent Signal Processing, 2007. WISP 2007, IEEE, pp. 1–5

6. Rahnamayan S, Tizhoosh HR (2008) Image thresholding using micro opposition-based differential evolution (micro-ODE). In: 2008 IEEE Congress on Evolutionary Computation (IEEE World Congress on Computational Intelligence), pp. 1409–1416

7. Hasan H, Haron H, Hashim SZ (2009) Freeman chain code extraction using differential evolution (DE) and particle swarm optimization (PSO). In: 2009. SOCPAR'09. International Conference of Soft Computing and Pattern Recognition, IEEE, pp. 77–81

8. Azarbad M, Ebrahimzadeh A, Babajani-Feremi A (2010) Brain tissue segmentation using an unsupervised clustering technique based on PSO algorithm. In: Biomedical Engineering (ICBME), 2010 17th Iranian Conference of, IEEE, pp. 1–6

9. Kumar S, Pant M, Ray AK (2011) Differential evolution embedded Otsu's method for optimized image thresholding. In: 2011 World Congress on Information and Communication Technologies (WICT), IEEE, pp. 325–329

10. Li Z, Chen X, Luo P, Tian Y (2012) Water area segmentation of the Yangcheng Lake with SAR data based on improved 2D maximum entropy and genetic algorithm. In: 2012 Second International Workshop on Earth Observation and Remote Sensing Applications (EORSA), IEEE, pp. 263–267

11. Sarkar S, Das S (2013) Multilevel image thresholding based on 2D histogram and maximum Tsallis entropy—a differential evolution approach. IEEE Trans Image Process 22(12):4788–4797

12. Paul S, Bandyopadhyay B (2014) A novel approach for image compression based on multi-level image thresholding using Shannon entropy and differential evolution. In: Students' Technology Symposium (TechSym), 2014 IEEE, pp. 56–61

13. Ochoa-Montiel R (2015) Thresholding of biological images by using evolutionary algorithms. In: 2015 Latin America Congress on Computational Intelligence (LA-CCI), IEEE, pp. 1–6

14. El Allaouil A, Nasri M, Merzougui M, Mirhisse J (2016) Evolutionary Algorithm for Segmentation of Medical Images by Region Rrowing. In: 2016 13th International Conference on Computer Graphics, Imaging and Visualization (CGiV), IEEE, pp. 119–124